

Towards New Half-Metallic Systems: Zinc-Blende Compounds of Transition Elements with N, P, As, Sb, S, Se, and Te

Iosif Galanakis and Phivos Mavropoulos*

Institut für Festkörperforschung, Forschungszentrum Jülich, D-52425 Jülich, Germany

(Dated: May 21, 2019)

We report systematic first-principles calculations for ordered zinc-blende compounds of the transition metal elements V, Cr, Mn with the *sp* elements N, P, As, Sb, S, Se, Te, motivated by recent fabrication of zinc-blende CrAs, CrSb, and MnAs. They show ferromagnetic half-metallic behavior for a wide range of lattice constants. We discuss the origin and trends of half-metallicity and examine the half-metallic behavior of their transition element terminated (001) surfaces.

PACS numbers: 71.20.Be, 71.20.Lp, 75.50.Cc

I. INTRODUCTION

The swiftly developing field of spin electronics¹ has provided strong motivation towards the construction of novel magnetic materials. Of particular interest are half-metals, *i.e.* compounds for which only the one spin direction presents a gap at the Fermi level E_F , while the other has a metallic character. Such behavior is present in various perovskite structures,² in Heusler compounds,³ and in dilute magnetic semiconductors.⁴ Lately it has been possible to grow binary CrAs in the zinc-blende (z-b) structure epitaxially on GaAs; this compound was found to be half metallic, both by experiment and by relevant calculations.⁵ It has also the great advantage of a high Curie temperature T_C , around 400 K.⁶ Similar is the T_C of ferromagnetic z-b CrSb.⁷ Moreover, the growth of nanoscale z-b MnAs dots on GaAs substrates⁸ has been achieved and CrAs/GaAs multilayers have been fabricated.⁹ Evidently, the know-how on the construction of these materials, which perhaps can be viewed as the limiting cases of dilute magnetic semiconductors, is increasing, and they will possibly be at the center of interest of spintronics applications soon, since they combine half-metallicity, high Curie temperature, and coherent growth on semiconductor (SC) substrates.

The experimental work on these systems seems to lie ahead of the theoretical analysis. Pioneering calculations concerning the bulk or the surfaces have been reported,^{5,10,11,12,13,14,15} but there is still extensive work to be done. One matter to be discussed is the origin of the half-metallicity; another is the question whether half-metallicity is preserved at the surfaces; and a third, in view of the future possible growth of similar compounds based on different SC or transition metals, is the theoretical prediction of the cases where half-metallicity can manifest itself, in order to serve as a helpful guideline to where future experiments can focus. It is the purpose of this paper to address these three points by first-principles calculations.

The outline of the paper has as follows. In Section II we shortly describe our method of calculation. In Section III we address the question of the origin of the half-metallic behavior and discuss the electronic structure of the z-

b compounds of transition elements with *sp* atoms. In Section IV we present the results of extensive systematic calculations for the z-b compounds of the form XY, with X=V, Cr, Mn, and Y=N, P, As, Sb, S, Se, Te, for various lattice constants in a ferromagnetic configuration, and we examine in which cases half-metallicity is present. In Section V we focus on the half-metallicity of transition metal terminated (001) surfaces. We conclude with a summary in Section VI.

II. METHOD OF CALCULATION

To perform the calculations, we have used the Vosko, Wilk and Nusair parameterization¹⁶ for the local density approximation (LDA) of the exchange-correlation potential to solve the Kohn-Sham equations within the full-potential screened Korringa-Kohn-Rostoker (KKR) Green function method,¹⁷ where the correct shape of the Wigner-Seitz cells is accounted for.¹⁸ To calculate the charge density, we integrate along a contour on the complex energy plane, which extends from below the $4s$ states of the *sp* atom up to the Fermi level, using 42 energy points. For the Brillouin zone (BZ) integration we have used a \mathbf{k} -space grid of $30 \times 30 \times 30$ in the full BZ for the bulk calculations and a \mathbf{k}_{\parallel} -space grid 30×30 in the two-dimensional full BZ for the surface calculations. We have used a cutoff of $\ell_{\max}=3$ for the wavefunctions and Green functions. More details on the surface calculations are described in Ref. 14.

The z-b structure can be easily seen to fit on a bcc lattice, by occupying only half of the sites with the two kinds of atoms and leaving the other half as voids. Viewed in this way, the consecutive lattice sites of bcc in the cubic diagonal are occupied by Ga, As, Void1, Void2 (in the case of *e.g.* GaAs). This is useful for the KKR method because all empty space of the quite open z-b structure is taken into account.

We must also say a few words about state-counting with the KKR method. The charge is found by adding the partial contributions of *s*, *p*, *d*, and *f* electrons (if a cutoff of $\ell_{\max}=3$ is used). In this way one ignores the contribution to the wavefunction of higher angular

momenta, which, although very small, is nonzero. This has a negligible effect for calculations in a metal, where the missing (or extra) charge is regained by a very small readjustment of the Fermi level E_F . However, if there is a band gap at E_F , one finds the charge to deviate slightly from the integer value it should have by state-counting. As a consequence for half metals, although the density of states (DOS) and the inspection of the bands show clearly that E_F lies within the gap for minority spin, and hence the magnetic moment per unit cell must be integer, its calculated value deviates slightly from the exact integer value. In our work, the presence of half metallicity has always been judged by inspection of the density of states and of the energy bands, and not from the value of the magnetic moment. The partial values of the charges and moments, calculated by local orbital summation, are accurate to within 1%.

III. ELECTRONIC STRUCTURE

In this section we shall examine the electronic structure of the compounds, and discuss the origin of the half metallicity and the value of the total moment. Although for arbitrary \mathbf{k} the wavefunctions do not belong exclusively to a single irreducible representation such as t_{2g} or e_g , it is convenient to retain this terminology for the bands formed by originally t_{2g} or e_g orbitals since they are rather separated. Let us focus on a $3d$ atom. In the z-b structure, the tetrahedral environment allows its t_{2g} states (d_{xy} , d_{yz} , and d_{zx}) to hybridize with the p states of the four first neighbors (the sp atoms). Note that in tetrahedral geometry, the p orbitals of the four neighboring sites transform as partners of the t_{2g} irreducible representation when analysed around the central site.²⁶ This creates a large bonding-antibonding splitting, with the low-lying bonding states being more of p character around the sp neighbors (we call these bands “ p -bands” henceforth), and the antibonding being rather of d character around the $3d$ atom. The gap formed in between is partly filled by the e_g states of the $3d$ atom (d_{z^2} and $d_{x^2-y^2}$); the position of the gap will be different for majority and minority electrons, due to the exchange splitting.

The situation can be elucidated by examination of the energy bands of CrAs, presented in Fig. 1. The s states of As are very low in energy and omitted in the figure. Around -3 eV, the p -bands can be seen. The next bands are the ones formed by the Cr e_g orbitals, around -1.5 eV for majority and $+1$ eV for minority. They are quite flat, reflecting the fact that their hybridization with the states of As neighbors is weak (or even zero, at $\mathbf{k} = 0$, due to symmetry). These bands can accommodate two electrons per spin. Above them, the substantially wider antibonding p - t_{2g} hybrids appear, starting from -1 eV for majority and from $+1.5$ eV for minority. Their large bandwidth can be attributed to the strong hybridization and to their high energy position. The bonding-antibonding splitting

is also contributing to the fact that they be pushed up beyond the flat e_g states. As a result, the three families of bands do not intermix, but are rather energetically separate. In the majority-spin direction the bonding-antibonding splitting is smaller, because the transition element $3d$ states are originally lower in energy, closer to the p states of the sp atom. In the minority spin direction the states are higher due to the exchange splitting and the gap is around E_F . Band counting gives an integer total magnetic moment of $3 \mu_B$.

To the clear bonding-antibonding gap also the z-b geometry contributes, since it has been previously reported^{10,12,13} that in the hexagonal NiAs geometry MnP, MnAs and MnSb show no gap.

Here we must refer to two recent publications on zincblende MnAs¹⁰, and MnP, MnAs, and MnSb,¹² which have identified the p and t_{2g} bands the other way around; *i.e.* they claim that the bonding bands are more of d -character around Mn and the antibonding more of p character around the sp atom. We believe that to be a small misinterpretation, at least for the minority spin, and present in favor of our interpretation the atom-projected density of states for MnAs in Fig. 2. Especially for the minority-spin direction, the antibonding states have almost all of their weight at the $3d$ atom. The bonding states have slightly more weight at the sp atom, while they also penetrate the Wigner-Seitz cell of the $3d$ atom and add weight there due to the large extension of the p orbitals. In the majority spin direction, on the other hand, the Mn $3d$ states are originally much lower, reaching the p states of the sp atoms. So, the hybridization is stronger and the character of the bonding bands can indeed be more d -like. As for the other $3d$ atoms considered here (Cr and V), they have higher-lying d states than Mn, so that the p character of the bonding states increases. Apart from this point, our line of analysis agrees with the one given in Refs. 10 and 12.

Next we consider different compounds, to see the trend of increasing transition metal atomic number: VAs, CrAs, MnAs. The corresponding DOS can be seen in Fig. 2, calculated for the InAs lattice parameter in all cases to allow comparison. For VAs, E_F lies between the majority e_g and t_{2g} . Since they are separated, this results in zero DOS at E_F , as in the limiting case of a semiconductor with almost zero band gap. The moment is $2 \mu_B$. As the number of valence $3d$ electrons increases for CrAs, the t_{2g} bands are pulled down enough to accommodate one electron ($M = 3 \mu_B$), and for MnAs even more, so as to accommodate two electrons, whence $M = 4 \mu_B$. At the same time, for the minority spin the band gap does not change in magnitude and continues to embrace E_F . This can be understood in terms of the exchange splitting ΔE_x being proportional to the magnetic moment: $\Delta E_x \simeq IM$. When the moment increases by $1 \mu_B$, ΔE_x must increase by one time the exchange integral I , about 0.8 eV. Thus the minority bands remain almost at their position.

This behavior is quite stable, unless the energy gained

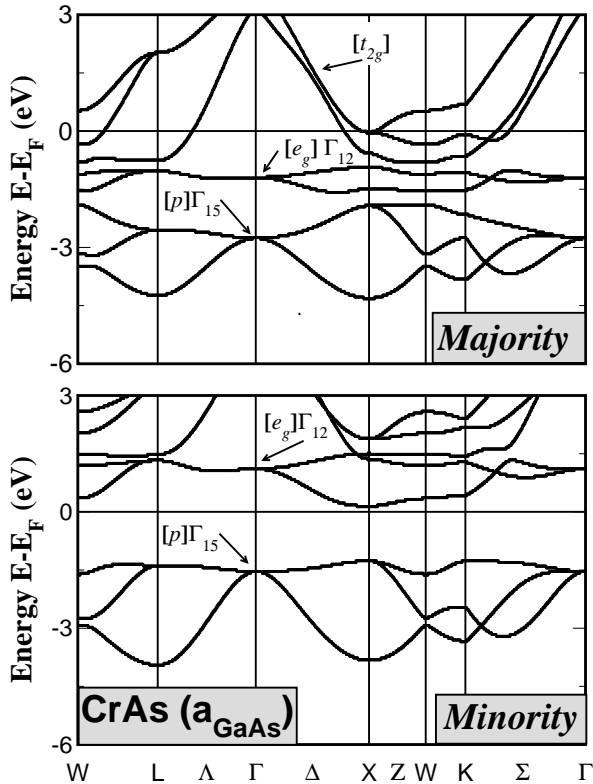


FIG. 1: Energy bands of CrAs calculated in the GaAs lattice constant. With p , e_g , and t_{2g} we denote the whole bands originating from orbitals of the corresponding character, although this character is well defined only for $\mathbf{k} = 0$. The bonding-antibonding splitting between the p and t_{2g} bands is evident; the band gap is between the p and the flat e_g bands. The system is half-metallic.

by increasing the exchange splitting in order to achieve one more μ_B is overshoot by the Coulomb energy cost; remember that the majority t_{2g} bands are wide. Then the system compromises by placing E_F higher, within the minority e_g conduction band, and half metallicity is lost. This can occur for small lattice constants or at the surface, and will be presented in the next sections.

Generally, the bonding p bands can accommodate 6 electrons (3 per spin), and since they lie low in energy they must be filled up; in addition, there is yet another band lower in energy, consisting of the s states of the sp atom, which has space for two electrons (one per spin). Once these 8 bands are filled by 8 of the valence electrons, the remaining electrons will fill part of majority d states, first the lower-lying e_g and then the t_{2g} , creating the magnetic moment. This electron counting gives then an integer total moment of

$$M = (Z_{\text{tot}} - 8) \mu_B, \quad (1)$$

where Z_{tot} is the total number of valence electrons in the unit cell.²⁷ This “rule of 8” is the analogue of the Slater-Pauling behavior for these systems; similar behavior is

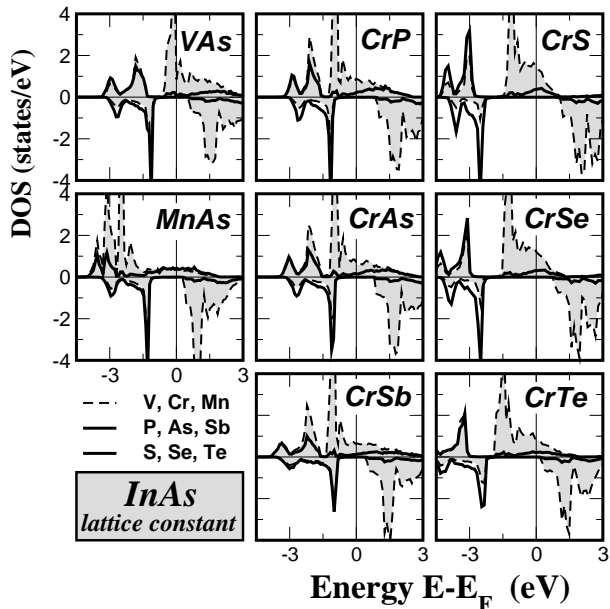


FIG. 2: Atom-resolved DOS for several materials in the z -b structure using the InAs lattice constant. Negative numbers on the DOS axis represent the minority spin. The dashed lines containing the shadowed area correspond to the DOS within the Wigner-Seitz cell of the transition element, while the full lines to the one of the sp atom. The small DOS of the vacant sites is omitted. In all cases, E_F lies within the minority-spin gap, *i.e.* the systems are half-metallic. Spin moments for these compounds are given in Table I.

found in the case of the half-metallic Heusler alloys, as a “rule of 18” or a “rule of 24”.^{19,20} Of course these are valid only when half-metallicity is present.

According to the “rule of 8” of Eq. (1), the (integer) moment should increase by 1 μ_B if one changes only the sp atom from group V to group VI, since then one more valence electron is available (in this respect there is a similarity to the dilute magnetic semiconductors²¹). In order to present this, we calculated the electronic structure of the $3d$ -group VI compounds. In Fig. 2 the DOS of CrS, CrSe, and CrTe are shown. We chose to use the InAs lattice constant in this case, so as to compare with the group V compounds at a single lattice constant. Note that the InAs lattice (6.058Å) is very close to the CdSe one (6.052Å). We found a ferromagnetic half-metallic solution for these cases, with a magnetic moment of 4 μ_B as expected. The physical mechanism involved is the same as in the $3d$ -group V case, and the main difference lies in that p states of the group VI elements lie lower in energy, so that the band gap is larger and the hybridization with the neighbor d states smaller.

We have also calculated the $3d$ -group VI compounds VS, VSe, VTe, MnS, MnSe, and MnTe. They also show half-metallic behavior for a range of lattice constants, with their magnetic moment given by the “rule of 8”;

TABLE I: Spin magnetic moment in μ_B for the InAs experimental lattice constant. The atomic-resolved moment values refer to the moment included in a Wigner-Seitz cell around each atom. Void1 and Void2 refer to the vacant sites used to describe the zinc-blende structure as described in Section II. The total moment does not appear exactly integer as explained in Section II.

| Compound | 3dat. | <i>sp</i> -at. | Void1 | Void2 | Total |
|----------|-------|----------------|--------|-------|-------|
| CrN | 3.887 | -1.071 | 0.027 | 0.127 | 2.960 |
| CrP | 3.318 | -0.448 | -0.019 | 0.085 | 2.935 |
| CrAs | 3.269 | -0.382 | -0.029 | 0.080 | 2.937 |
| CrSb | 3.148 | -0.249 | -0.036 | 0.084 | 2.946 |
| VAs | 2.054 | -0.196 | 0.006 | 0.076 | 1.939 |
| MnAs | 4.070 | -0.250 | 0.008 | 0.106 | 3.935 |
| CrS | 3.858 | -0.117 | 0.050 | 0.154 | 3.945 |
| CrSe | 3.830 | -0.102 | 0.050 | 0.162 | 3.939 |
| CrTe | 3.752 | -0.057 | 0.053 | 0.182 | 3.930 |
| VSe | 2.750 | -0.054 | 0.068 | 0.173 | 2.937 |
| MnSe | 4.579 | 0.149 | 0.061 | 0.142 | 4.931 |

they will be discussed in the next section. However, we must note that we have only searched for the ferromagnetic solution. A systematic investigation of the energetics of ferromagnetic *vs.* antiferromagnetic solutions lies beyond the scope of this paper. Especially in the case of Mn-group VI compounds, an antiferromagnetic solution could be possible, since these compounds are iso-electronic with FeAs, which has been found to have an antiferromagnetic ground state at the equilibrium lattice constant in calculations by Shirai.¹¹ For the compounds VAs, CrAs, and MnAs, the analysis of Shirai points towards stable ferromagnetic solutions.

In Table I the magnetic moments are presented for several *3d*-group V and *3d*-group VI materials for the InAs lattice constants. All these compounds are half-metallic, even MnSe, where the t_{2g} majority spin band is filled completely to achieve the $5 \mu_B$. The total moment, calculated by summation over KKR local orbitals instead of state counting, does not appear exactly integer as it should, as explained in Section II.

From Table I we see that the *sp* atom has an induced local magnetic moment M_{loc} opposite to the one of the *d* atom. This is in agreement with previous results on *3d*-As compounds.^{10,11,12} The trend is that for lighter *sp* elements the induced moment absolute value increases (M_{loc} becomes more negative); for the group VI elements (higher ionicity) these effects are smaller. This behavior can be understood in the following way. In the case of *3d*-Group V compounds, the minority *p* band is more located within the Wigner-Seitz cell of the *sp* atom, whereas the majority *p* band is more hybridized with the low *d* orbitals and thus more shared with the *3d* atoms; this results in the opposite magnetic moments of the *sp* atoms. For lighter elements the *p* wavefunctions are more localized, but this localization affects more the minority than the majority electrons, again because of the hybridization of the latter with the low *d* orbitals of the *3d* atoms

(this is evident in the DOS of CrSb, CrAs, and CrP in Fig. 2). Thus the absolute value of the local moment on the *sp* atoms is stronger for the lighter elements. Naturally, the local moment also increases the *3d* atom since the minority-spin weight added to the *sp* atom is taken from the *3d*, and the total magnetic moment must remain a constant integer. In the case of *3d*-Group VI compounds, the antiparallel moment of the *sp* atom and the change for lighter elements is smaller, because the *p* states are deeper in energy, thus less hybridized with the transition element majority *d* states and more alike for the two spin directions.

Another effect of going to lighter *sp* elements is the increase of the band gap, as can be seen in Fig. 2 for CrSb→CrAs→CrP and CrTe→CrSe→CrS. This is consistent with the picture that the local magnetic moment of the *3d* atom increases, causing a larger exchange splitting ΔE_x and pushing up the minority e_g bands.

IV. VARIATION OF LATTICE CONSTANT

The compounds consisting of *3d* and *sp* elements that have been fabricated^{5,7,8} are metastable in the *z*-b structure. For instance, MnAs is grown in orthorhombic or hexagonal structure,²² in which it does not present half-metallic behavior,^{10,12} although it is still ferromagnetic. The metastable *z*-b structure can be achieved only when the materials are grown on top of a *z*-b semiconductor, such as GaAs.^{5,7,8} It can be expected that in the first few monolayers the materials will adopt the lattice constant of the underlying buffer; thus, the question arises whether half-metallicity is present for the lattice parameter of the semiconductor. To peruse this, we have performed calculations of all combinations of the type XY with X=V, Cr, Mn, and Y=N, P, As, Sb, for the lattice constants of the relevant *z*-b III-V semiconductors GaN, InN, GaP, GaAs, InP, InAs, GaSb, and InSb (given in increasing lattice parameter order).

Our results are summarized in Table II. A “+” sign means that the compound is half-metallic for the given lattice constant, while a “-” sign means loss of half-metallicity. A \pm means that though the system is not half metallic, the spin polarization at E_F is very close to 100%. Where half-metallicity is preserved, the total magnetic moment is given by Eq. (1). Note that even in the cases where half-metallicity is lost, a *p*-*d* hybridization gap is present (but not at E_F). Upon compression, the bandwidth of the valence *p*-bands and the e_g bands increases and the gap between them decreases somewhat — the increase of the bonding-antibonding splitting is not relevant, since it concerns the relative position of the *p* and t_{2g} bands. Most importantly, though, E_F is shifted towards higher energies by the majority states, so that it can step into the minority e_g band and destroy half-metallicity. In Table II we see that all materials examined are half-metallic for the large lattice constant of InSb, but lose the half-metallicity for the small one of

TABLE II: Calculated properties of different materials adopting the zinc-blende structure using the experimental lattice constants a of several z-b III-V semiconductors. A “+” sign means that a system is half-metallic, a “-” that the Fermi level is above the gap and a “ \pm ” that the Fermi level is only slightly within the conduction band and the spin polarization at E_F is almost 100%. The experimental lattice parameters were taken from Refs. 23,24 except for the case of GaN and InN in the zinc-blende structure which were taken from Refs. 23,25.

| | a(Å) | GaN | InN | GaP | GaAs | InP | InAs | GaSb | InSb |
|----------|------|------|------|------|------|------|-------|------|------|
| Compound | 4.51 | 4.98 | 5.45 | 5.65 | 5.87 | 6.06 | 6.10 | 6.48 | |
| VN | - | - | + | + | + | + | + | + | + |
| VP | - | - | - | + | + | + | + | + | + |
| VAs | - | - | - | + | + | + | + | + | + |
| VSb | - | - | - | - | + | + | + | + | + |
| CrN | - | + | + | + | + | + | + | + | + |
| CrP | - | - | - | + | + | + | + | + | + |
| CrAs | - | - | - | + | + | + | + | + | + |
| CrSb | - | - | - | - | + | + | + | + | + |
| MnN | - | + | + | + | + | + | + | + | + |
| MnP | - | - | - | - | + | + | + | + | + |
| MnAs | - | - | - | - | + | + | + | + | + |
| MnSb | - | - | - | - | - | - | \pm | + | + |

TABLE III: Similar to Table II for transition metal compounds with the group VI elements. The experimental lattice parameters were taken from Ref. 23.

| | a(Å) | ZnS | ZnSe | CdS | CdSe | ZnTe | CdTe |
|----------|------|-------|-------|------|-------|-------|------|
| Compound | 5.41 | 5.67 | 5.82 | 6.05 | 6.10 | 6.49 | |
| VS | - | - | + | + | + | + | + |
| VSe | - | - | - | + | + | + | + |
| VTe | - | - | - | - | \pm | \pm | + |
| CrS | - | + | + | + | + | + | + |
| CrSe | - | \pm | + | + | + | + | + |
| CrTe | - | - | - | + | + | + | + |
| MnS | - | + | + | + | + | + | + |
| MnSe | - | - | \pm | + | + | + | + |
| MnTe | - | - | - | - | - | - | + |

GaN.

The general trend observed in Table II, apart from the effect of compression, is that the tendency towards half-metallicity increases for lighter sp elements. This is consistent with the picture that for lighter group V elements the p state is energetically lower and also more localized. Both these factors result in reducing the shifting of E_F by compression; but more importantly, the gap increases for lighter sp elements as analyzed at the end of Sec. III. Thus half-metallicity holds out longer.

Similar trends are observed in the case of $3d$ -group VI compounds. The systematics are presented in Table III. The investigated systems are XY with X=V, Cr, and Mn, and Y=S, Se, and Te, for the experimental lattice constants of the II-VI semiconductors ZnS, ZnSe, CdS, CdSe, ZnTe, and CdTe. Again we see the loss of half-metallicity by compression, and a stronger tendency

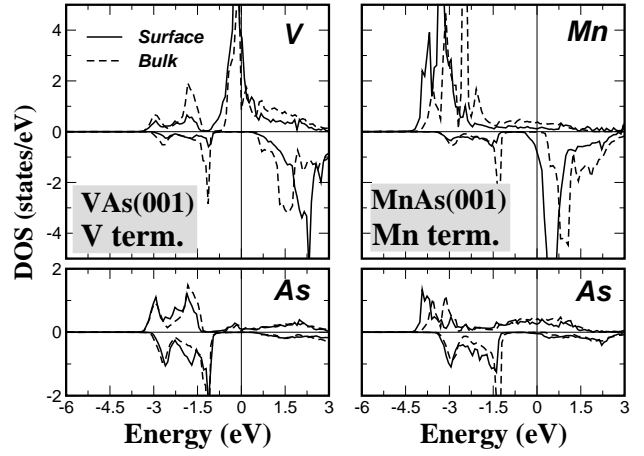


FIG. 3: Left panel: Spin- and atom-resolved DOS of the V-terminated (001) surface for the V atom at the surface layer and the As atom at the subsurface layer for the InAs lattice constant (left panel). The surface DOS (full lines) and the bulk DOS (dashed lines) are shown. The As s states are located at around 10 eV below the Fermi level and are not shown in the figures. The energy zero refers to E_F ; negative numbers on the DOS axis represent the minority spin. Right panel: Same for the Mn-terminated MnAs (001) surface.

towards half-metallicity for lighter group VI elements; both effects can be attributed to the same reasons as in the $3d$ -group V case.

V. (001) SURFACES

In the last part of this paper we examine the possibility of half-metallicity at the surfaces of these compounds. One of the authors (IG) has recently studied the (001) surface of CrAs.¹⁴ The conclusion of that study was that the As terminated surface loses the half-metallicity due to As dangling bonds that form a surface band within the minority spin gap, while the Cr terminated surface retains the half-metallic character and the local magnetic moment increases. This behavior was found for both the GaAs and InAs lattice constants. Here we have extended our calculations to include the VAs and MnAs (001) surfaces, for the InAs lattice constant. Since for the As terminated surfaces the surface states originating from dangling bonds cannot be avoided, we will discuss the termination with the $3d$ atom. Although at the surface the t_{2g} and e_g representations are no longer relevant (the former splits in two, one containing $d_{xz} + d_{yz}$ and one d_{xy} , and the latter also in two, one containing $d_{x^2-y^2}$ and one d_{z^2}), we ask for understanding that we continue to use the same terminology in order to make the connection to the bulk states.

The DOS for the VAs and MnAs (001) surfaces are shown in Fig. 3, for both the atom at the surface layer (V or Mn) and at the subsurface layer (As). For comparison, the corresponding DOS in the bulk are also pre-

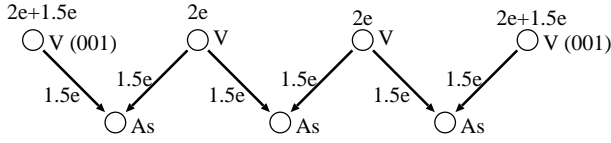


FIG. 4: Schematic interpretation of the origin of the excess moment of $1.5 \mu_B$ at the VAs surface. The arrows represent the donation of V electrons to the valence band generated mainly by the low-lying As p orbitals. At the V-terminated (001) surface, half the neighbors of the V atom are missing, so an excess of 1.5 electrons remains. They occupy the majority-spin states, giving an extra $1.5 \mu_B$. The situation is similar in all $3d$ -group V compounds; for the $3d$ -group VI compounds the p band welcomes in total 2 instead of 3 electrons from each $3d$ atom, thus the excess moment is 1 instead of $1.5 \mu_B$.

sented. Evidently the V terminated VAs (001) surface remains half-metallic. However, there is an important difference in the DOS as compared to the bulk case, especially at the surface (V) layer. For the majority spin, the peak at around -2 eV is strongly reduced, and the same happens for the minority spin at around -1 eV. This can be explained by the fact that the surface V atom has a reduced coordination number of only two As neighbors. Then two less As p orbitals penetrate the V cell, reducing the local weight of the bonding states. At the same time, the majority peak just under the Fermi level is enhanced, gaining the weight which has been lost by the bonding states from both spin directions. Note in the DOS of the V surface atom that there is no more the clear minimum at E_F for the majority states, which was distinguishing e_g from t_{2g} in the bulk, as the reduced bonding-antibonding splitting allows the latter states to come lower in energy.

In terms of electron counting, the V atoms in the bulk give away 3 of the 5 valence electrons to the p band and retain the remaining two to build up the magnetic moment. Due to the reduced coordination at the surface, only 1.5 electron per V atom is given away, thus 3.5 remain to fill up majority states and build up the magnetic moment; due to the gap, minority states cannot take over any of these extra electrons, unless E_F moves higher into the e_g -like band (this is the case for Mn to which we shall turn shortly). The situation is given schematically in Fig. 4.

In this way there is a transfer of weight from minority to majority electrons under E_F , the magnetic moment increases, and therefore the exchange splitting becomes larger, pushing the minority antibonding and e_g -like states higher in energy. In this respect, the shift of the minority peak above E_F from 1.5 eV (bulk) to 2.2 eV (surface) can be explained; otherwise the gap could have decreased due to reduced hybridization. The increased magnetic moment must reach $3.5 \mu_B$ in the vicinity of the surface; we find that $3.07 \mu_B$ are located on the surface layer, about $0.35 \mu_B$ in the vacuum, and the rest adds up to the moment of the subsurface layer. We see

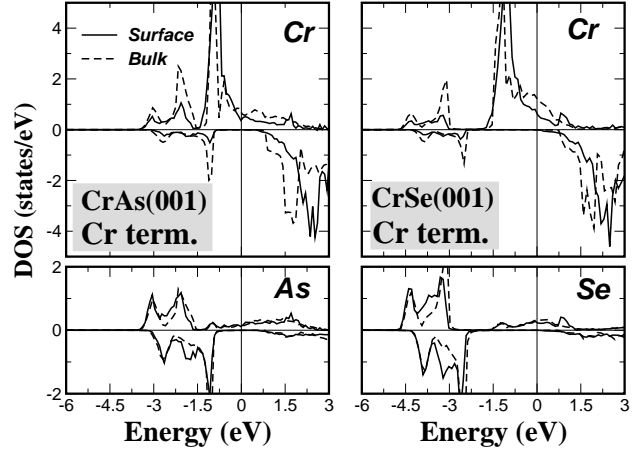


FIG. 5: Spin- and atom-resolved DOS of the Cr-terminated CrAs and CrSe (001) surfaces for the Cr atom at the surface layer and the As and Se atoms at the subsurface layer for the InAs lattice constant. The As and Se s states are located at around 10 eV below the Fermi level and are not shown in the figures. The surface DOS are compared to the bulk calculations (dashed lines). The energy zero refers to E_F ; negative numbers on the DOS axis represent the minority spin.

that the integer value of the magnetic moment, which is mandatory in bulk half-metallicity, ceases to be a prerequisite in the vicinity of the surface.

The situation described here is completely analogous to the one of the CrAs (001) surface.¹⁴ There, the magnetic moment of the surface layer was reported to reach $4 \mu_B$; if the magnetic moment of the vacuum and the subsurface layer is added, one finds a total moment of $4.5 \mu_B$ in the vicinity of the surface, *i.e.* $1.5 \mu_B$ more than in the bulk.

However, things are different for MnAs (001) (with Mn termination). The corresponding DOS of the surface Mn atom and of the subsurface As atom is shown in Fig. 3 (right panel). Manifestly, half-metallicity has been lost. The difference to the VAs and CrAs cases lies in the high magnetic moment of $4 \mu_B$ that MnAs already shows in the bulk. If its moment were to increase by the same mechanism and remain half-metallic, the surface (plus vacuum and subsurface layers) would have to accommodate 5.5 majority spin electrons. This is energetically unfavorable, since the extra half electron cannot be accommodated by the t_{2g} band, so that higher-lying bands would have to be populated. Instead, as the majority states are lowered, the slow gain in magnetic moment is not enough to increase the exchange splitting substantially, and the minority d states also reach E_F . As a net result, majority and minority DOS peaks are substantially lower in energy, half-metallicity is lost, and a total magnetic moment of $4.59 \mu_B$ is present within the first surface layer.

We have also made calculations for the X terminated XSe(001) surfaces, where X=V, Cr, and Mn, using the InAs lattice constant. The V and Cr ones are half-metallic while the Mn surface is not half-metallic. The

arguments in the above paragraphs still hold, but now each V, Mn or Cr atom loses Se (group VI) neighbors instead of As (group V) and thus the electron counting changes. In the bulk each X atom gives away only 2 electrons to the p band and not 3 as in the XAs compounds. Losing two neighbors means that the surface X atom gives away now only 1 electron, so we should have now 4 electrons for V or 5 electrons for Cr to build up the spin moment, *i.e.* we should have $1 \mu_B$ more than in the bulk. Indeed we find the total spin moment to increase to $4 \mu_B$ for VSe(001) and $5 \mu_B$ for CrSe(001). The MnSe compound cannot be half-metallic as this would mean a total spin moment of $6 \mu_B$ at the surface which is energetically unfavourable for reasons similar to the MnAs surface.

A comparison of the CrAs(001) with the CrSe(001) surface DOS, both Cr terminated and at the InAs lattice constant, is shown in Fig. 5, where the bulk DOS is also presented. We see that the differences in the bulk of the two materials (larger gap, more weight in the majority states under E_F to account for one more electron) remain their major differences also in the surfaces.

VI. SUMMARY AND CONCLUSION

We have studied zinc-blende compounds of the transition metal elements V, Cr, Mn with the group V sp elements N, P, As, Sb and the group VI S, Se, Te, in the ferromagnetic configuration. They all show a tendency towards half-metallic behavior, *i.e.* 100% spin polarization at E_F . This can be traced back to the bonding-antibonding splitting due to hybridization between the transition element d (t_{2g}) states and the sp element p states, conspiring with the large exchange splitting which pushes up the minority d states. The total moment per unit cell, if the system is half-metallic, is integer and given by the “rule of 8”. Also, the sp atoms are found to have an antiparallel local moment with respect to the $3d$

atoms; the absolute value of the local moments increases for lighter or less ionized sp elements. This is traced back to the degree of localization of the p wavefunctions around the sp atoms.

We have discussed the trends with varying lattice constant, in view of the possibility to grow these materials epitaxially on various semiconductors. Compression eventually kills half-metallicity, since E_F finally wanders above the minority gap. However, for compounds involving lighter sp elements half-metallicity is encouragingly more robust; this can be explained in terms of the stronger local moment close to the $3d$ atom for lighter sp elements, resulting in a larger exchange splitting and gap.

Finally, we have examined the behavior of the transition element terminated (001) surfaces. In most cases half metallicity is maintained, and the magnetic moment increases because of the missing neighbours where charge would be transferred. Exceptions are the cases where the surface magnetic moment should exceed $5 \mu_B$, for which half metallicity is lost.

In view of recent experimental success to grow such compounds, and of their relevance to the field of spintronics, we believe that our work will not only add to the understanding of these systems, but will also contribute to the future realization of spintronics devices.

Acknowledgments

Financial support from the RT Network of *Computational Magnetoelectronics* (contract RTN1-1999-00145) of the European Commission is gratefully acknowledged. The authors would like to thank Professor P. H. Dederichs for helpful discussions and for a critical reading of the manuscript. Motivating discussions with Professor H. Katayama-Yoshida and Dr. K. Sato are also gratefully acknowledged.

* Electronic address: Ph.Mavropoulos@fz-juelich.de

¹ G. A. Prinz, *Science* **282**, 1660 (1998).

² R. J. Soulen Jr., J. M. Byers, M. S. Osofsky, B. Nadgorny, T. Ambrose, S. F. Cheng, P. R. Broussard, C. T. Tanaka, J. Nowak, J. S. Moodera, A. Barry, and J. M. D. Coey, *Science* **282**, 85 (1998).

³ R. A. de Groot, F. M. Mueller, P. G. van Engen, and K. H. J. Buschow, *Phys. Rev. Lett.* **50**, 2024 (1983).

⁴ F. Matsukura, H. Ohno, A. Shen, and Y. Sugawara, *Phys. Rev. B* **57**, R2037 (1998).

⁵ H. Akinaga, T. Manago, and M. Shirai, *Jpn. J. Appl. Phys.* **39**, L1118 (2000).

⁶ M. Mizuguchi, H. Akinaga, T. Manago, K. Ono, M. Oshima, and M. Shirai, *J. Magn. Magn. Mater.* **239**, 269 (2002).

⁷ J. H. Zhao, F. Matsukura, K. Takamura, E. Abe, D. Chiba, and H. Ohno, *Appl. Phys. Lett.* **79**, 2776 (2001).

⁸ K. Ono, J. Okabayashi, M. Mizuguchi, M. Oshima, A. Fujimori, and H. Akinaga, *J. Appl. Phys.* **91**, 8088 (2002).

⁹ M. Mizuguchi, H. Akinaga, T. Manago, K. Ono, M. Oshima, M. Shirai, M. Yuri, H. J. Lin, H. H. Hsieh, and C. T. Chen, *J. Appl. Phys.* **91**, 7917 (2002).

¹⁰ S. Sanvito and N. A. Hill, *Phys. Rev. B* **62**, 15553 (2000).

¹¹ M. Shirai, *Physica E* **10**, 143 (2001).

¹² A. Continenza, S. Picozzi, W. T. Geng, and A. J. Freeman, *Phys. Rev. B* **64**, 085204 (2001).

¹³ Y.-J. Zhao, W. T. Geng, A. J. Freeman, and B. Delley, *Phys. Rev. B* **65**, 113202 (2002).

¹⁴ I. Galanakis, *Phys. Rev. B* **66**, 012406 (2002).

¹⁵ B.-G. Liu (unpublished); preprint in arXiv:condmat/0206485

¹⁶ S. H. Vosko, L. Wilk, and N. Nusair, *Can. J. Phys.* **58**, 1200 (1980).

¹⁷ N. Papanikolaou, R. Zeller, P. H. Dederichs, *J. Phys.: Con-*

- dens. Matter **14**, 2799 (2002).
- ¹⁸ N. Stefanou, H. Akai, and R. Zeller, *Comp. Phys. Commun.* **60**, 231 (1990); N. Stefanou and R. Zeller, *J. Phys.: Condens. Matter* **3**, 7599 (1991).
- ¹⁹ I. Galanakis, N. Papanikolaou, and P. H. Dederichs, *Phys. Rev. B* *to be published*; Preprint in *arXiv:cond-mat/0203534*.
- ²⁰ I. Galanakis, N. Papanikolaou, and P. H. Dederichs, *Phys. Rev. B* *to be published*; Preprint in *arXiv:cond-mat/0205129*.
- ²¹ K. Sato (private communication).
- ²² V. M. Kaganer, B. Jenichen, F. Schippan, W. Braun, L. Däweritz, and K. H. Ploog, *Phys. Rev. Lett.* **85**, 341 (2000)
- ²³ Landolt-Börnstein, New Series, Group III, Vol. 17, Pt.a edited by O. Madelung, Springer-Verlag, Berlin (1982).
- ²⁴ Landolt-Börnstein, New Series, Group III, Vol. 22, Pt.a edited by O. Madelung, Springer-Verlag, Berlin (1986).
- ²⁵ Landolt-Börnstein, New Series, Group III, Vol. 41, Pt.A1a edited by U Rössler, Springer-Verlag, Berlin (2001).
- ²⁶ Again, this is strict only for $\mathbf{k} = 0$
- ²⁷ The cumbersome electron counting can be avoided by just observing that $M = N_{\text{maj}} - N_{\text{min}} = N_{\text{maj}} + N_{\text{min}} - 2 \times N_{\text{min}} = Z_{\text{tot}} - 2 \times N_{\text{min}}$, where N_{maj} and N_{min} are respectively the numbers of majority and minority valence electrons.